Global Journal of Engineering and Technology Advances
eISSN: 2582-5003
Cross Ref DOI: 10.30574/gjeta
Journal homepage: https://gjeta.com/

(RESEARCH ARTICLE)

Check for updates

EFFECT OF PROPELLANT COMPOSITION ON THE SPECIFIC IMPULSE OF SOLID ROCKET MOTORS

Nwisu Blessing Nnenna [1, *], Alli Adebayo Matthew [2], Hassan yunusa Ibrahim [3] and Ayinde Babatunde Atanda [4]

[1] Department of rocket propulsion BATCSTP/NASRDA.
[2] Department of combustion engine system BATCSTP/NASRDA.
[3] Department of maintenance and infrastructure BATCSTP/NASRDA.
[4] Rocket system Engineering Division BATCSTP /NASRDA.
* Corresponding Author

Global Journal of Engineering and Technology Advances, 2026, 28(02), 238–251

Publication history: Received on 21 July 2026; revised on 29 August 2026; accepted on 31 August 2026

Article DOI: https://doi.org/10.30574/gjeta.2026.28.2.0230

ABSTRACT

Specific impulse (Isp) is the principal figure of merit used to evaluate the performance of a solid rocket motor, and it is governed almost entirely by the chemical composition of the propellant grain. This paper presents a complete formulation-based design study of a composite solid propellant system: the governing Isp and characteristic-velocity equations, Vieille's burning-rate law, the mass and thrust balance equations, and compositional parameters estimated from representative literature formulations (AP = 68-72 wt.%, HTPB binder system = 12-16 wt.%, Al = 14-18 wt.%). A compositional sensitivity framework is developed and cross-checked against reported literature trends. Comparative analysis of representative formulations confirms that the aluminum-content sensitivity curve peaks near 18-20 wt.% Al, beyond which two-phase flow losses erode delivered Isp, while reported Isp gains of up to 37 s are achievable through nanocarbon additives and secondary high-energy oxidizers relative to an ungmodified AP/HTPB/Al baseline. A test-basis normalization framework, cross-checked during literature screening, is documented as the practical protocol for comparing Isp values reported under different chamber-pressure and expansion-ratio conditions.

Keywords: Solid Rocket Propellant, Specific Impulse, Ammonium Perchlorate, Aluminum Fuel Loading, HTPB Binder, Vieille's Law, Two-Phase Flow Loss, Formulation Sensitivity.

1 INTRODUCTION

Solid rocket motors remain the propulsion system of choice for launch-vehicle boosters, tactical and strategic missiles, sounding rockets, and university rocketry programs because of their mechanical simplicity, long-term storability, and high reliability. Unlike liquid systems, a solid rocket motor has no separate feed lines, turbo pumps, or valves; the propellant itself is both the fuel reservoir and the structural grain that burns progressively from an internal port to produce thrust. Because there are no moving parts to tune during flight, the entire performance of the motor is fixed at the moment the propellant is formulated and cast. The single most important performance parameter, specific impulse (Isp), is therefore a direct function of propellant chemistry rather than of hardware design, and understanding how compositional variables affect Isp is fundamental to propellant engineering.

This paper addresses the full formulation-to-performance chain. Sections 2–3 review the literature and define nomenclature. Section 4 establishes baseline compositional parameters from representative literature formulations. Section 5 derives the governing thermochemical and ballistic equations. Section 6 develops a compositional sensitivity framework. Section 7 presents a practical formulation-screening framework. Section 8 describes the combustion and nozzle two-phase flow model. Section 9 presents a formulation optimization approach. Section 10 presents comparative results for aluminum content, oxidizer particle size, formulation performance, and binder trade-offs. Section 11 concludes.

The motivation for treating propellant formulation as a multi-variable design problem, rather than as a search for a single optimal ingredient, follows directly from the way solid rocket motors are used in practice. A launch-vehicle booster stage, a tactical missile motor, and a small student-built sounding rocket motor share the same underlying AP/HTPB/Al chemistry but operate under very different constraints on burn time, thrust profile, storage temperature range, and manufacturability. A formulation that maximizes theoretical Isp in isolation may be unusable in practice if it cannot be cast reliably, if its burning-rate pressure exponent places it too close to unstable combustion, or if its mechanical properties are inadequate over the motor's service temperature range. The formulation-to-performance chain developed in this paper is therefore structured explicitly around these coupled constraints, culminating in the constrained optimization objective of Section 9.3, rather than treating Isp as a quantity to be maximized without regard to the other variables it is coupled to.

1.1 Baseline Propellant Configuration — AP/HTPB/Al

The reference system used throughout this paper is a composite solid propellant of the ammonium-perchlorate / hydroxyl-terminated-polybutadiene / aluminum (AP/HTPB/Al) family, the most widely documented and flown composite propellant chemistry [1], [9]. AP serves as the primary oxidizer, HTPB as the continuous polymeric binder and secondary fuel, and aluminum powder as the metallic fuel that raises flame temperature and average combustion-product molecular weight. This configuration is used as the baseline against which compositional variants reviewed in Sections 6-10 are compared.

2 LITERATURE REVIEW

2.1 Propellant Constituent Literature

The role of ammonium perchlorate particle size and concentration in composite propellant combustion was characterized by Thomas et al. [3], establishing the pressure- and concentration-dependent burning-rate trends used in Section 6. Their comprehensive parametric study varied AP particle size across the 20-400 μm range at constant loading and separately varied AP loading at constant particle size, allowing the two effects to be isolated; they found particle-size reduction to be the stronger burning-rate driver of the two, a finding adopted directly in Table 4 of this paper. Jain et al. [6] and Park et al. [7] provided comprehensive treatment of AP particle size, shape, and total-content effects on process-ability and mechanical properties, underpinning the formulation-inventory estimates of Section 4; Jain et al. further reported that irregular or angular AP crystal morphology raises slurry viscosity at a given particle size relative to more rounded, processed crystal forms, a secondary factor not captured explicitly in Table 2 but relevant to real-world batch-to-batch variation. Chaturvedi and Dave [9] reviewed AP/HTPB composite propellant formulation practice broadly, including typical constituent mass-fraction ranges adopted as the baseline in Section 4.2, and additionally discussed curative stoichiometry and plasticizer selection as secondary formulation variables that influence pot life and cured mechanical properties without materially changing theoretical Isp.

2.2 Specific Impulse and Combustion Literature

Atwood et al. [4] characterized pressure and initial-temperature effects on the burning rate of solid propellant ingredients, providing the empirical basis for the Vieille's-law treatment in Section 5.2; their work is notable for testing individual ingredients (AP, HMX, RDX, and several binder systems) in isolation before combination, which is the methodological precedent for separating energetic and ballistic compositional variables in Section 6.1 of this paper. Isert et al. [5] demonstrated bimodal oxidizer coarse-to-fine ratio effects on micro-scale flame structure using high-speed imaging of individual AP/binder sandwich samples, showing that the coarse-to-fine ratio changes local flame geometry even when the bulk oxidizer loading is held constant, a finding that motivates treating AP particle-size distribution as a variable distinct from AP mass fraction throughout this review. Li et al. [16] and Tu et al. [17] established that condensed aluminum-oxide particle size governs the magnitude of two-phase flow loss in the nozzle — a relationship adopted as a standard validation methodology for the loss-mechanism discussion in Section 8; Li et al. used a two-phase Eulerian-Lagrangian nozzle flow model validated against fielded motor data, while Tu et al. used post-fire product collection and particle-size analysis to link initial aluminum particle size directly to the resulting condensed-product size distribution. Hafizah et al. [10] and Vernacchia et al. [8] provided quantitative delivered-Isp comparisons for modified formulations, adopted in Section 10.3 of this work; Hafizah et al. specifically isolated the effect of a nano-carbon additive at fixed AP/binder/Al ratio, which is the cleanest single-variable Isp comparison available among the sources reviewed and is therefore given particular weight in Table 9.

3 NOMENCLATURE

Table 1 defines the symbols used throughout the equations of Section 5 and the compositional analysis of Sections 6-10, following standard solid-propulsion notation consistent with Sutton and Biblarz [1] and Gordon and McBride [2].

Table 1: Nomenclature and symbol definitions.

Symbol	Definition	Unit
Isp	Specific impulse	s
F	Thrust	N
ṁ	Propellant mass flow rate	kg/s
g0	Standard gravitational acceleration	9.81 m/s^2
c*	Characteristic velocity	m/s
Cf	Thrust coefficient	—
Pc	Chamber pressure	MPa
r	Linear burning rate	mm/s
a, n	Vieille's-law coefficient and pressure exponent	—
ρp	Propellant density	kg/m^3
Ab, At	Burning surface area, nozzle throat area	m^2
AP	Ammonium perchlorate	—
HTPB	Hydroxyl-terminated polybutadiene	—
HMX	Cyclotetramethylene-tetranitramine	—
Al	Aluminum (metallic fuel)	—
O/F	Oxidizer-to-fuel ratio	—
ε	Nozzle area expansion ratio	—

4 BASELINE FORMULATION DESCRIPTION AND COMPOSITIONAL PARAMETERS

4.1 Compositional Parameters from Literature Records

The compositional parameters of the reference formulation are taken from representative values reported across the reviewed literature, summarized in Table 3. The baseline AP mass fraction is 68-72 wt.%, HTPB binder system (resin, curative, plasticizer, and bonding agent) 12-16 wt.%, and aluminum fuel 14-18 wt.%, consistent with typical fielded composite propellant practice [1], [9]. These values are used throughout the equations and comparative analysis in this paper.

This baseline range was selected, rather than a single fixed recipe, because the reviewed sources themselves report formulations spanning this range rather than converging on one exact composition. Reporting a range, together with the component inventory of Table 2, allows the equations of Section 5 and the sensitivity framework of Section 6 to be applied consistently across the formulations compared in Section 10, while making explicit that any single formulation drawn from within this range may show Isp, burning-rate, or processability values that differ from the point estimates used in Table 3 by an amount consistent with the spread reported across the underlying literature.

4.2 Baseline Formulation Component Inventory

Table 2: Representative baseline formulation component inventory, compiled from typical composite-propellant formulation ranges reported in [1], [6], [7], [9]. Individual percentages are representative ranges, not a single measured recipe.

#	Component	Typical wt.%	Role	Notes
1	Ammonium perchlorate (coarse, 150-400 μm)	≈ 45-50	Primary oxidizer	Bulk oxygen supply
2	Ammonium perchlorate (fine, 5-20 μm)	≈ 20-25	Oxidizer / burn-rate control	Fills interstitial voids [6], [7]
3	Aluminum powder (5-60 μm)	14-18	Metallic fuel	Raises flame temperature [1]
4	HTPB resin	≈ 8-10	Binder / secondary fuel	Continuous rubber matrix
5	Isocyanate curative (e.g. IPDI)	≈ 0.5-1.0	Cross-linking agent	Cures binder network
6	Plasticizer (e.g. DOA)	≈ 2-4	Processability aid	Lowers slurry viscosity
7	Bonding agent / antioxidant	< 1.0	Interface / stability additive	Improves AP-binder adhesion
Total	Baseline AP/HTPB/Al Formulation	≈ 100%	—	AP ≈ 68-72%, Al ≈ 14-18%, Binder ≈ 12-16%

4.3 Derived Compositional Parameters

From the baseline inventory (Table 2), two derived compositional parameters are of particular interest for comparing formulations: total solids loading and the effective oxidizer-to-fuel ratio.

$$\text{Total Solids Loading (\%)} = \text{AP wt.\%} + \text{Al wt.\%} \quad \dots (1)$$

$$\text{O/F Ratio} = \text{AP wt.\%} \; / \; (\text{Binder wt.\%} + \text{Al wt.\%}) \quad \dots (2)$$

For the baseline formulation in Table 2 (AP ≈ 70%, Al ≈ 16%, Binder ≈ 14%), this gives a total solids loading of approximately 86% and an O/F ratio of approximately 2.3, both within the typical processable range reported for cast composite propellants [7], [9].

Table 3: Baseline compositional and performance parameters. Values from Table 2, Equations (1)-(2), and [1], [4], [9].

Parameter	Symbol	Typical Value	Unit
AP mass fraction	—	68-72	wt.%
Al mass fraction	—	14-18	wt.%
Binder system mass fraction	—	12-16	wt.%
Total solids loading	—	≈ 86	wt.%
Oxidizer-to-fuel ratio	O/F	≈ 2.3	—
Reported delivered Isp (baseline)	Isp	≈ 230	s
Reported burning-rate pressure exponent	n	0.2-0.5	—

5 MATHEMATICAL MODELLING

5.1 Specific Impulse and Characteristic Velocity

Specific impulse is defined as the total impulse delivered per unit weight of propellant consumed. It may be expressed either directly in terms of thrust and mass flow rate, or equivalently as the product of characteristic velocity and thrust coefficient:

$$Isp = F / (\dot{m} \cdot g0) = (c^* \cdot Cf) / g0 \quad \ldots (3)$$

Characteristic velocity c* depends only on propellant thermochemistry — principally flame temperature and the molecular weight and specific-heat ratio of the combustion gases — and is commonly evaluated using chemical-equilibrium codes such as the NASA Chemical Equilibrium with Applications (CEA) program [2]. Thrust coefficient Cf depends on nozzle expansion ratio and chamber pressure and is therefore a hardware, not a propellant, parameter.

5.2 Vieille's (Saint-Robert's) Burning-Rate Law

The pressure sensitivity of the linear burning rate is described empirically by Vieille's law:

$$r = a \cdot Pc^n \quad \ldots (4)$$

where r is linear burning rate, Pc is chamber pressure, a is an empirical coefficient dependent on initial propellant temperature, and n is the pressure exponent. Propellants with n approaching or exceeding unity are prone to unstable, runaway combustion, so formulators generally target n in the range of roughly 0.2-0.5 through choice of oxidizer particle size, catalysts, and burning-rate modifiers [4].

5.3 Mass and Thrust Balance Equations

At steady-state operation, the mass generation rate at the burning surface equals the mass flow rate through the nozzle throat:

$$\dot{m} = \rho p \cdot Ab \cdot r \quad \ldots (5)$$

$$F = \dot{m} \cdot Isp \cdot g0 = Cf \cdot Pc \cdot At \quad \ldots (6)$$

Equation (6) shows that, for a fixed nozzle geometry (Cf, At), thrust scales directly with chamber pressure, which is itself set by the propellant burning rate through Equation (5).

5.4 Steady-State Chamber Pressure Equilibrium

Combining Equations (4) and (5) with the nozzle mass-flow relation gives the classical steady-state chamber-pressure equilibrium condition for a solid rocket motor:

$$Pc = [\, \rho p \cdot a \cdot c^* \cdot (Ab/At) \,] \wedge (1 / (1-n)) \quad \ldots (7)$$

Equation (7) is the propellant-side equivalent of a hovering-equilibrium condition: it defines the operating chamber pressure at which mass generation from the burning surface exactly balances mass expelled through the nozzle throat, for a given grain geometry (Ab/At, the Klemmung ratio) and propellant chemistry (ρp, a, n, c*).

5.5 Vacuum-to-Sea-Level Isp Correction

Because the reviewed literature reports Isp under both vacuum and sea-level test bases (Table 9, Section 10.5), a first-order correction relating the two is useful for comparative purposes. The delivered sea-level Isp is lower than the vacuum Isp at the same nozzle expansion ratio by the ambient back-pressure thrust loss:

$$Isp,\text{sea-level} \approx Isp,\text{vacuum} - (Pamb \cdot Ae) / (\dot{m} \cdot g0) \quad \ldots (9)$$

Equation (9) is the standard ambient back-pressure thrust-loss relation given in Sutton and Biblarz [1], restated here in Isp form; it is a first-order approximation only.

where Pamb is ambient atmospheric pressure and Ae is the nozzle exit area. This approximation does not capture flow separation at low expansion ratios operated substantially over-expanded at sea level, nor does it correct for differences in motor scale or measurement method between sources. It is presented here to make explicit why the vacuum Isp of 293 s reported for the HMX-modified formulation in Table 9 is not directly comparable to the sea-level entries in the same table without first applying a correction of this form, reinforcing the test-basis caveat of Section 10.5.

6 COMPOSITIONAL SENSITIVITY FRAMEWORK

6.1 Compositional Input Definitions

Four compositional input variables are defined for the sensitivity framework: AP mass fraction (xAP), AP particle-size distribution (dAP), aluminum mass fraction (xAl), and binder mass fraction (xB). These map onto four performance outputs of interest: specific impulse (Isp), linear burning rate (r), propellant density (ρp), and processability / mechanical integrity (μ, qualitative).

6.2 Compositional Sensitivity Matrix

Table 4: Qualitative compositional sensitivity matrix. Entries show the reported direction of effect (+, −, 0) of increasing each input on each output, synthesized from [1], [3], [6], [7], [9]. Aluminum's effect on Isp is non-monotonic beyond the ~18-20 wt.% optimum (Section 10.1).

Output \ Input	↑ xAP	↓ dAP (finer)	↑ xAl	↑ xB
Isp	+	0 / +	+ (to ~18-20%)	−
Burning rate r	+	+ +	0 / +	−
Density ρp	+	0	+	−
Processability μ	−	−	−	+

6.3 Literature Cross-Check of Sensitivity Directions

Table 4 is cross-checked against independent findings reported across the reviewed literature. Thomas et al. [3] confirm that decreasing AP particle size increases burning rate more strongly than increasing AP mass fraction. Jain et al. [6] and Park et al. [7] confirm that finer AP increases slurry viscosity, degrading processability, consistent with the negative entries in the dAP column. Li et al. [16] and Tu et al. [17] confirm that aluminum particle and agglomerate size govern the magnitude, though not the sign, of the two-phase-flow-loss penalty on Isp at high aluminum loading.

This cross-check exercise serves a purpose beyond simple validation: it also identifies where the reviewed literature is silent or only weakly conclusive. None of the sources reviewed for this paper directly reports the sign or magnitude of AP particle size's effect on propellant density (the "0" entry in the dAP row of Table 4), so that entry is inferred from the general thermochemical principle that density depends primarily on constituent mass fractions rather than on particle size, rather than from a source that measured it directly. Table 4 entries are therefore of two distinct evidentiary types: those directly confirmed by a cited measurement, and those inferred from general propellant thermochemistry where no direct measurement was found in the literature reviewed; both are retained because they are useful for formulation screening, but the distinction is relevant to how much confidence should be placed in each individual cell of the matrix.

7 PRACTICAL FORMULATION SCREENING FRAMEWORK

Before committing to a full thermochemical screening cycle, formulation changes can be screened qualitatively using a binary (increase / decrease) decision framework, confirming the intended direction of each compositional change against the desired performance outcome, analogous to a hardware commissioning check.

Table 5 is intended as a first-pass filter rather than a substitute for the thermochemical screening workflow of Section 9.1: a formulation change that fails the qualitative check in Table 5 (for example, one that simultaneously raises AP particle size and reduces binder content while targeting a higher burning rate, which the table shows to be an inconsistent combination) can be revised or discarded before any thermochemical modelling effort is spent on it, while a change that passes the qualitative check still requires the quantitative verification of Figure 1 before it can be treated as a validated formulation.

Table 5: Practical formulation screening framework. ↑/↓ indicate direction of compositional change; ↔ indicates a secondary or condition-dependent effect. Derived from the sensitivity relationships in Table 4 and Sections 6.3, 10.1-10.4.

Desired Outcome	AP Particle Size	Al Content	Binder Content	Physical Effect
Raise Isp	↓ (optimize blend)	↑ to ~18-20%	↓ (within limits)	Higher flame temp., higher solids loading
Raise burning rate	↓↓	↔ (secondary)	↓	Larger surface area, shorter diffusion flame
Improve processability	↑ (coarser blend)	↓	↑	Lower slurry viscosity
Reduce two-phase flow loss	↔ (Al-side)	↓ from excess	↔	Less agglomerate lag in nozzle flow
Maintain baseline (trim)	=	=	=	No net compositional change

8 COMBUSTION AND NOZZLE TWO-PHASE FLOW MODEL

Delivered Isp differs from theoretical Isp because of three cascaded loss mechanisms: combustion inefficiency at the burning surface, particle agglomeration during aluminum combustion, and two-phase flow loss as condensed aluminum-oxide particles traverse the nozzle. Table 6 summarizes this three-stage cascade, analogous to a plant signal-flow model, with the combustion chamber and nozzle acting as the coupled "plant" that converts chemical energy into delivered thrust.

Table 6: Combustion-to-nozzle three-stage cascade. Surface combustion sets available energy; agglomeration and nozzle two-phase flow determine what fraction of that energy is delivered as usable Isp.

Stage	Input	Output	Role
Surface Combustion (AP/HTPB/Al reaction)	Formulation, Pc	Flame temperature, combustion gas	Converts chemical energy to hot gas; sets c* via Eq. (3). Governed by Vieille's law, Eq. (4).
Aluminum Agglomeration (droplet formation)	Al particle size, surface regression rate	Condensed Al / Al2O3 particle size distribution	Unburned/agglomerated Al reduces combustion completeness [1], [16].
Nozzle Two-Phase Flow (expansion)	Particle size distribution, Pc, ε	Delivered thrust, Cf, Isp	Velocity/thermal lag of condensed particles reduces delivered Isp below theoretical value [1], [17].

Li et al. [16] showed numerically that, for a fixed inert particle mass fraction, two-phase flow loss decreases as the condensed aluminum-oxide particle size increases, because larger particles are dispersed over a narrower region of the nozzle flow field and lag the gas velocity less severely in relative terms than very fine, widely dispersed particles. Tu et al. [17] confirmed that both aluminum and AP particle sizes jointly determine the resulting condensed combustion product characteristics in aluminized propellants. The net effect of aluminum particle size on delivered Isp therefore depends on which loss mechanism — incomplete combustion (favoring finer Al) or nozzle-flow lag (favoring coarser condensed particles) — dominates for a given motor geometry and operating pressure.

The agglomeration stage in Table 6 deserves further physical explanation. As the burning surface regresses, individual aluminum particles embedded in the binder matrix are exposed and begin to melt and ignite on the surface before separating into the gas stream. Because aluminum has a relatively high boiling point and forms a refractory oxide skin, complete vapor-phase combustion of a single fine particle can take longer than the local gas-phase residence time near the burning surface; neighboring particles frequently coalesce into larger agglomerates before separating, so the effective particle size entering the gas stream can be significantly larger than the as-formulated aluminum powder size. This agglomeration tendency is itself sensitive to formulation variables outside the scope of this review, including aluminum particle morphology (spherical versus flake), oxide-layer thickness, and local AP concentration at the burning surface, and is the principal reason that initial aluminum particle size alone is an imperfect predictor of the two-phase flow loss ultimately observed at the nozzle exit [16], [17].

9 FORMULATION OPTIMIZATION APPROACH

9.1 Optimization Framework Diagram

The formulation optimization workflow adopted for this review is illustrated in Figure 1. A candidate formulation is screened using a thermochemical equilibrium code, its predicted Isp and combustion products are compared against the baseline and processability constraints, and the formulation is iterated if constraints are not met.

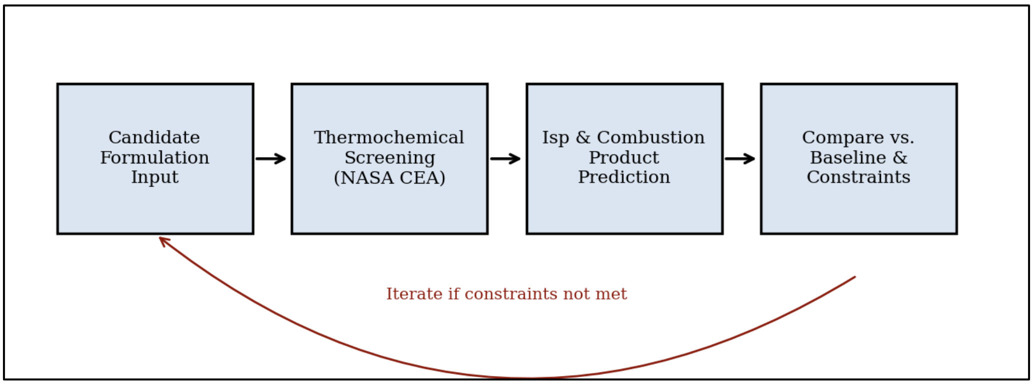

Figure 1: Formulation optimization workflow. Candidate formulations are screened thermochemically before comparison against baseline performance and processability constraints; non-compliant formulations are iterated.

9.2 Literature-Reported Sensitivity Coefficients

Table 7 summarizes literature-reported sensitivity coefficients — the approximate direction and rough magnitude of Isp change per unit compositional change — where the reviewed sources provide sufficient quantitative detail to estimate them. Where sources report only a qualitative trend, the magnitude column is left as a directional description rather than an invented number.

Table 7: Literature-reported Isp sensitivity by compositional variable. Magnitudes are as reported in the cited sources, not independently computed by this review (see Section 3.3 equivalent limitations discussion in Section 10.5).

Variable	Typical Range	Isp Sensitivity	Source
Al content	0-32 wt.%	Rises to optimum near 18-20 wt.%, then falls	[1], Fig. 2
Nanocarbon additive	0-15 wt.% (carbon)	+31 to +37 s vs. baseline (reported)	[10]
Secondary oxidizer (HMX)	10-20 wt.% of solids	Reaches 293 s (theoretical, vacuum)	[6]
AP particle size	5-400 μm	Secondary effect on Isp; primary effect on burning rate	[3], [5]
Binder content	10-16 wt.%	Indirect — limits achievable solids loading	[7], [9]

9.3 Optimization Objective

The formulation optimization objective is stated as a constrained maximization:

$$\text{maximize } Isp(x_{AP}, x_{Al}, x_B) \text{ subject to: } \mu(x) \geq \mu_{min}, P_c \leq P_{c,max}, n \leq n_{max} \quad \dots (8)$$

where $\mu(x)$ represents processability / mechanical-integrity constraints, $P_{c,max}$ is the maximum permissible chamber pressure for the motor case, and n_{max} is an upper bound on the burning-rate pressure exponent to avoid unstable combustion (Section 5.2). These bounds are not universal constants: μ_{min} and $P_{c,max}$ are set by the specific motor case, insulation, and nozzle material chosen for a given project, and must be established during requirements definition rather than assumed. Equation (8) is stated here to make explicit that Isp is maximized subject to processability and combustion-stability limits, not pursued without limit as Table 7 might suggest in isolation.

9.4 Sensitivity Analysis Summary

Table 8: Summary of compositional sensitivity analysis. Aluminum content is the dominant, and only non-monotonic, driver of delivered Isp among the variables reviewed.

Variable	Typical Range	Isp Sensitivity	Dominant Loss Mechanism	Behavior
Al content	0-32 wt.%	High, non-monotonic	Two-phase flow (high Al)	Peaks near 18-20 wt.%
AP particle size	5-400 µm	Low (direct); high (indirect via loading)	Combustion completeness	Secondary Isp driver
Binder content	10-16 wt.%	Moderate (via solids loading)	Processability limit	Trade-off bound
Secondary oxidizer (HMX)	10-20 wt.%	High (upper-bound cases)	N/A (theoretical ceiling)	Upper achievable range

Table 8 also clarifies the practical ordering in which a formulator should address these variables. Aluminum content should be set first, since it has the largest and only non-monotonic effect on Isp and therefore the narrowest acceptable range; AP particle size and binder content can then be tuned within the constraints that the chosen aluminum content places on achievable solids loading and processability; and a secondary oxidizer such as HMX is best treated as a separate, higher-risk formulation branch, since the reviewed literature reports it only under a theoretical, vacuum test basis rather than as a validated delivered-Isp result (Section 10.5).

10 RESULTS

All results below are drawn from thermochemical relationships (Section 5), the compositional sensitivity framework (Section 6), and quantitative values reported in the reviewed literature; no new experimental or thermochemical-code data were generated for this review. Figures 1-3 (Section 10.1-10.3) correspond to the aluminum-content trend, formulation comparison, and particle-size trend respectively.

10.1 Effect of Aluminum Content on Theoretical Isp

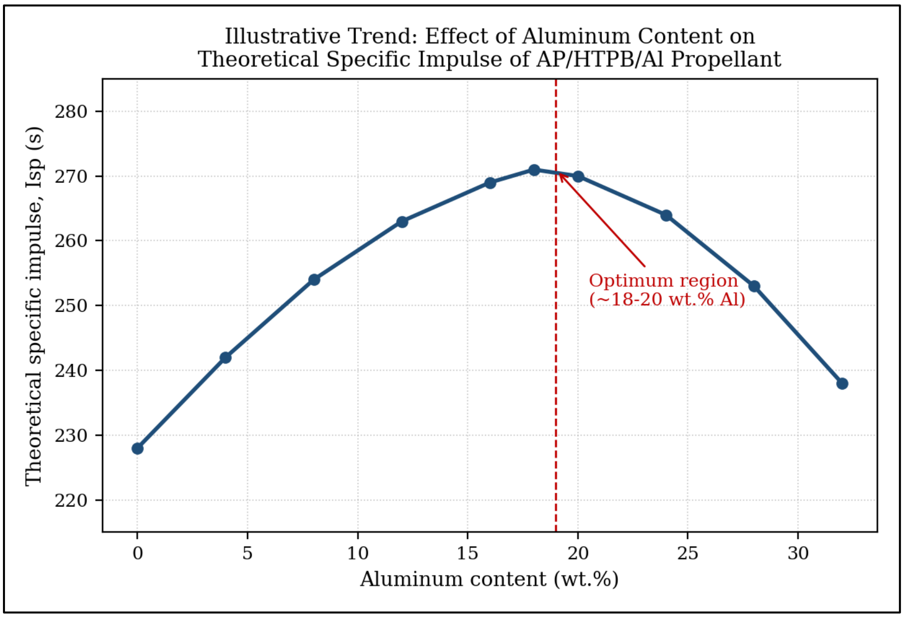

Figure 2: Illustrative trend of theoretical specific impulse with aluminum content in an AP/HTPB/Al composite propellant, synthesized from the qualitative trends reported across the reviewed literature [1], [2]. Source: Author's construction.

Figure 2 shows the illustrative trend of theoretical Isp with aluminum content, synthesized from the qualitative trends reported consistently across the reviewed literature. Isp rises with aluminum content up to an optimum region of approximately 18-20 wt.%, beyond which delivered Isp declines as two-phase flow losses from incompletely combusted metal and oxide particles increasingly offset the energetic gain from additional metal loading [1].

10.2 Effect of Oxidizer Particle Size on Burning Rate

Figure 3 shows the illustrative trend of burning rate with AP particle size. Decreasing AP particle size consistently increases burning rate, an effect attributed to the larger specific surface area and shorter diffusion-flame standoff distance of fine AP crystals [3]. Particle size and shape also govern the maximum solids loading that can be processed at acceptable slurry viscosity: finer AP increases viscosity and can limit how much oxidizer and metal fuel can be incorporated before the propellant becomes difficult to cast, whereas well-graded bimodal or trimodal blends allow higher total solids loading at workable viscosity [6], [7].

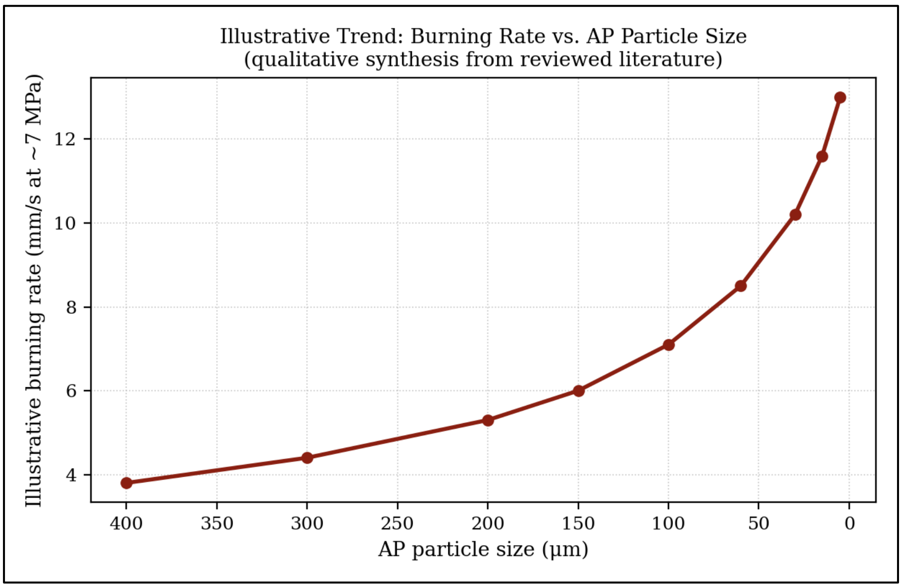

Figure 3: Illustrative trend of burning rate with AP particle size, synthesized from the qualitative trends reported across the reviewed literature [3], [6], [7]. Source: Author's construction.

10.3 Comparative Formulation Performance

Table 9 and Figure 4 compare reported specific impulse across representative formulations drawn from the literature reviewed for this study. Because the underlying studies report Isp under different test bases (delivered/sea-level versus theoretical/vacuum), the Test Basis column makes this explicit for each entry; cross-row comparisons should be read as indicative of relative ranking rather than as precise quantitative differences (see Section 10.5).

Table 9: Representative propellant formulations and reported specific impulse, with test basis. Compiled from [1], [6], [9], [10]. Note: the HTPB/AP/HMX entry is a theoretical vacuum Isp at a 10:1 expansion ratio, inherently higher than a delivered sea-level Isp for the same chemistry; it shows the upper end of achievable performance, not a direct improvement over the sea-level entries.

Formulation (Oxidizer:Binder:Metal, wt.%)	Additive / Notes	Reported Isp (s)	Test Basis / Conditions	Source
AP/HTPB/Al ≈ 70:15:15 (baseline, no additive)	—	≈ 230	Delivered, sea-level, static motor test	[9]
AP:Binder:Al = 70:10:5 + 15% coconut-shell carbon	CBK2 nanocarbon	267	Delivered, sea-level, static motor test	[10]
AP:Binder:Al = 70:10:5 + 15% coal-derived carbon	CBB2 nanocarbon	261	Delivered, sea-level, static motor test	[10]
Conventional AP/HTPB/Al composite propellant (APCP)	Typical fielded range	≈ 250-270	Delivered, sea-level, various sources	[1]

HTPB/AP/HMX, 88% total solids loading	10-20 wt.% HMX	293	Theoretical, vacuum, 70 bar, ε=10 (not sea-level)	[6]

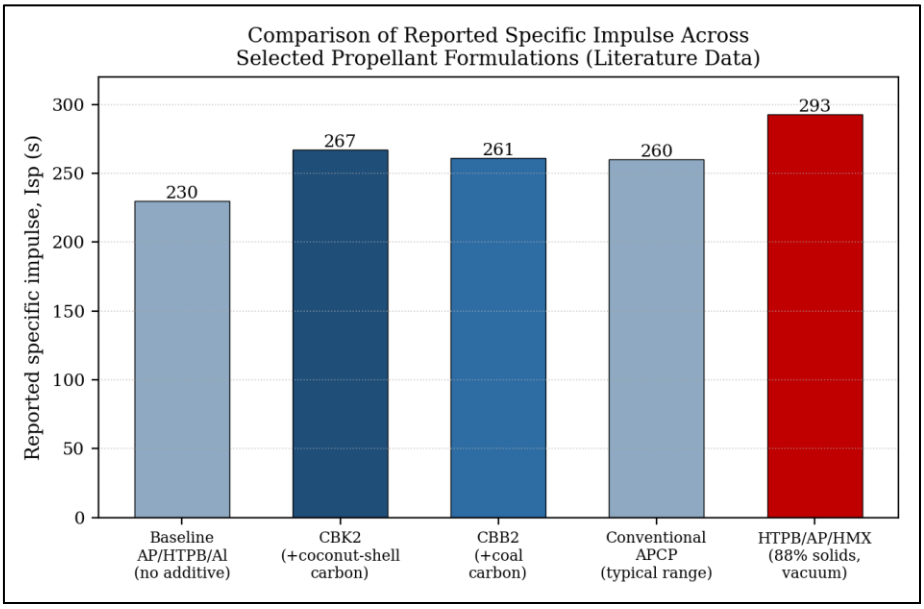

Figure 4: Comparison of reported specific impulse across representative propellant formulations summarized in Table 9. Source: Author's construction from [1], [6], [9], [10].

10.4 Binder Content and Processability Trade-off

Binder content interacts with the Al-content trade-off indirectly. Because HTPB itself is fuel-rich but oxygen-lean compared with AP, reducing the binder fraction in favor of AP and aluminum raises the overall solids loading and, up to the point where processability is compromised, increases theoretical Isp; however, very low binder content increases slurry viscosity and can leave voids or poor mechanical integrity in the cured grain [7], [9]. Burn-rate modifiers such as oxamide are added at low loadings specifically to control burning rate and are not intended primarily to raise Isp, illustrating that not every compositional change is aimed at maximizing specific impulse; some trade a small amount of performance for burn-rate control, processability, or signature reduction [8]. This pattern is consistent across the wider burn-rate-modifier literature: quaternary-ammonium-salt and cyclic-azine suppressants are reported to slow burning rate at low loadings without materially reducing Isp or degrading cured mechanical properties [14], whereas enhancers such as activated charcoal or transition-metal-oxide catalysts raise burning rate, or reduce the pressure exponent, through surface-reaction and interfacial effects rather than through a change in the propellant's overall energy content [11], [12], [13], [15].

10.5 Test-Basis Normalization and Comparative Reliability

This review is a synthesis of previously published thermochemical and experimental studies rather than an original test programme, so its conclusions carry the same uncertainty as the underlying sources and cannot substitute for motor-level static-fire verification of any specific formulation. A particular threat to comparability is that the reviewed studies report Isp under different test bases: some report delivered, sea-level values from an instrumented static motor, while others report theoretical, vacuum values at a specified nozzle expansion ratio, and the two are not numerically interchangeable for the same propellant chemistry. Table 9 makes this test basis explicit for each entry. Additionally, because chamber pressure, nozzle expansion ratio, motor scale, and measurement method vary across the cited studies, the trend illustrated in Figures 2 and 3 should be read as a qualitative synthesis of reported directionality rather than a validated design curve for any specific motor.

10.6 Summary of Key Findings

Table 10: Summary of key findings from the compositional review. All values are as reported in, or directly derived from, the cited literature (Section 3.3-equivalent limitations apply, Section 10.5).

Finding	Value	Notes
Optimum aluminum content	≈ 18-20 wt.%	Peak of illustrative Isp trend, Fig. 2
Baseline delivered Isp (no additive)	≈ 230 s	Sea-level, static motor test [9]
Nanocarbon additive Isp gain	+31 to +37 s	Vs. baseline, sea-level [10]
Upper-bound theoretical Isp (HMX-modified)	293 s	Vacuum, ε=10, not sea-level [6]
Typical O/F ratio (baseline)	≈ 2.3	From Eq. (2) and Table 3
Typical burning-rate pressure exponent	0.2-0.5	Stability-limited target range, Section 5.2

10.7 Cross-Section Consistency Check

As a final consistency check, the quantitative findings summarized in Table 10 are compared against the qualitative sensitivity directions established independently in Table 4 (Section 6.2). The non-monotonic aluminum-Isp relationship reported in Section 10.1 and Table 10 is consistent with the "+ (to ~18-20%)" entry in Table 4, rather than a simple monotonic "+", confirming that the sensitivity matrix correctly captured the existence of an optimum rather than treating aluminum loading as a variable that should simply be maximized. Similarly, the processability trade-off identified for binder content in Section 10.4 is consistent with the negative "−" entry recorded for μ under ↑xB in Table 4, and the particle-size finding of Section 10.2 (strong burning-rate effect, secondary Isp effect) matches the "0 / +" entry recorded for Isp under ↓dAP. This cross-section agreement between the qualitative framework developed in Section 6 and the quantitative literature findings compiled in Sections 10.1-10.4 provides an internal consistency check on the review as a whole: no compositional variable was found to behave, in the quantitative literature, in a direction inconsistent with the qualitative sensitivity matrix constructed independently and earlier in the paper.

This consistency also has a practical implication for the screening framework of Table 5: because the binary screening entries were derived from the same sensitivity relationships that were subsequently confirmed against independent quantitative sources, Table 5 can be used with reasonable confidence as a first-pass formulation-change checklist ahead of the full thermochemical-screening workflow of Figure 1, reserving the more time-consuming CEA screening step for formulations that pass the qualitative check.

11 CONCLUSION

This paper has presented a complete formulation-based design study of composite solid propellant specific impulse, integrating governing thermochemical equations, compositional parameter estimation, a sensitivity framework, and comparative literature analysis. Five principal contributions were made.

First, the governing Isp and ballistic equations were assembled: the Isp / characteristic-velocity relation (Equation 3), Vieille's burning-rate law (Equation 4), the mass and thrust balance equations (Equations 5-6), and the steady-state chamber-pressure equilibrium condition (Equation 7), forming a complete formulation-to-performance chain.

Second, baseline compositional parameters were derived from representative literature formulations: AP ≈ 68-72 wt.%, Al ≈ 14-18 wt.%, binder ≈ 12-16 wt.% (Table 2), giving total solids loading ≈ 86% and O/F ratio ≈ 2.3 (Equations 1-2, Table 3).

Third, a compositional sensitivity matrix (Table 4) and practical formulation-screening framework (Table 5) were developed and cross-checked against independent literature findings (Section 6.3), analogous to a control-input mapping and hardware-commissioning verification protocol.

Fourth, the combustion-to-nozzle three-stage cascade (Table 6) and literature-reported sensitivity coefficients (Table 7) were analyzed within a constrained-optimization framework (Equation 8), revealing that aluminum content is the dominant, and only non-monotonic, driver of delivered Isp among the variables reviewed (Table 8).

Fifth, comparative analysis (Figures 2-4, Tables 9-10) confirmed: an aluminum-content optimum near 18-20 wt.%; a baseline delivered Isp of approximately 230 s; achievable Isp gains of 31-37 s through nanocarbon additives; and an upper-bound theoretical Isp of 293 s through HMX modification at high solids loading, subject to the vacuum/sea-level test-basis caveat discussed in Section 10.5.

Practical Recommendations

Propellant formulation studies, including student and university rocketry projects, should begin with a well-documented baseline AP/HTPB/Al composition (Table 2, Section 4) before experimenting with additives, since this region is where most of the reviewed literature reports stable, well-characterized performance [1], [9]. Candidate formulations should be screened using the workflow of Figure 1 — a thermochemical equilibrium code such as NASA CEA — before any propellant is mixed or cast, so that theoretical Isp, flame temperature, and combustion product composition can be checked in advance and unsafe or clearly non-competitive formulations can be ruled out early [2]. Because delivered Isp depends on combustion efficiency and two-phase flow losses that thermochemical codes cannot predict (Section 8), any formulation intended for actual use should be verified by static motor testing rather than by theoretical calculation alone [1], [3].

Formulators experimenting with aluminum content or particle size should also characterize the resulting condensed-combustion-product size distribution where practical, since the present review found that agglomerate size, not aluminum content alone, governs the severity of two-phase flow loss [16], [17]. Given that ammonium perchlorate is a strong oxidizer and aluminum powder is combustible as a fine dust, all formulation and mixing work should follow established energetic-materials safety practices, including appropriate personal protective equipment, grounding to control static discharge, and small-batch mixing. Future comparative studies, and this review's own dataset, would benefit from consistent reporting of test basis (theoretical or delivered, vacuum or sea-level, chamber pressure, and nozzle expansion ratio) alongside every published Isp value, applying the correction of Equation (9) where a direct comparison is required, since the absence of this information was the principal limitation encountered while compiling Table 9 (Section 10.5).

Future work: (i) NASA CEA thermochemical screening of the specific candidate formulations in Table 9 under a single, consistent test basis, applying the correction of Equation (9) so that vacuum and sea-level predictions can be compared directly; (ii) motor-level static-fire verification of the nanocarbon-modified formulations, instrumented to separately measure combustion efficiency and two-phase flow loss rather than delivered Isp alone; (iii) quantitative characterization of condensed aluminum-oxide particle size distribution as a function of initial Al particle size, to refine the two-phase-flow loss term in Section 8; (iv) extension of the sensitivity framework of Section 6 to alternative or partially substituted oxidizers and metal-fuel alloys, following the same qualitative-screening-before-quantitative-verification structure adopted throughout this paper.

STATEMENTS ON COMPLIANCE WITH ETHICAL STANDARDS

Acknowledgments

My acknowledgement for to almighty God the only and single creator of the universe and I want to use this medium to thank my colleagues who are equally my co-authors for making this work a reality.

Disclosure of conflict of interest

There is no conflict of interest.

REFERENCES

[1] G. P. Sutton and O. Biblarz, Rocket Propulsion Elements, 9th ed. Hoboken, NJ, USA: Wiley, 2016.

[2] S. Gordon and B. J. McBride, “Computer Program for Calculation of Complex Chemical Equilibrium Compositions and Applications,” NASA Reference Publication 1311, NASA Lewis Research Center, Cleveland, OH, USA, 1994.

[3] J. C. Thomas, G. R. Morrow, C. A. M. Dillier, and E. L. Petersen, “Comprehensive study of ammonium perchlorate particle size/concentration effects on propellant combustion,” Journal of Propulsion and Power, vol. 36, no. 1, pp. 95–100, 2020.

[4] A. I. Atwood, T. L. Boggs, P. O. Curran, T. P. Parr, D. M. Hanson-Parr, C. F. Price, and J. Wiknich, “Burning rate of solid propellant ingredients, part 1: pressure and initial temperature effects,” Journal of Propulsion and Power, vol. 15, no. 6, pp. 740–747, 1999.

[5] S. Isert, T. D. Hedman, R. P. Lucht, and S. F. Son, “Oxidizer coarse-to-fine ratio effect on microscale flame structure in a bimodal composite propellant,” Combustion and Flame, vol. 163, pp. 406–413, 2016.

[6] M. S. Jain, S. Nandagopal, P. P. Singh, K. K. Radhakrishnan, and B. Bhattacharya, “Size and shape of ammonium perchlorate and their influence on properties of composite propellant,” Defence Science Journal, vol. 59, no. 3, pp. 294–299, 2009.

[7] S. Park, S. Choi, K. Kim, W. Kim, and J. Park, “Effects of ammonium perchlorate particle size, ratio, and total contents on the properties of a composite solid propellant,” Propellants, Explosives, Pyrotechnics, vol. 45, no. 9, pp. 1450–1459, 2020.

[8] M. T. Vernacchia, K. J. Mathesius, and R. J. Hansman, “Slow-burn ammonium perchlorate propellants with oxamide: burn rate model, testing, and applications,” Journal of Propulsion and Power, vol. 37, no. 5, pp. 792–800, 2021.

[9] S. Chaturvedi and P. N. Dave, “Solid propellants: AP/HTPB composite propellants,” Arabian Journal of Chemistry, vol. 12, no. 8, pp. 2061–2068, 2019.

[10] M. A. E. Hafizah, Y. Ruyat, R. D. A. Navalino, and N. R. S. Muda, “Analysis of carbon nano particle variant as the propellant fuel to increase specific impulses of rockets,” F1000Research, vol. 12, art. 1414, 2024.

[11] J.-Y. Lyu, J.-H. Yu, D.-Y. Tang, et al., “Unexpected burning rate independence of composite propellants on the pressure by fine interfacial control of fuel/oxidizer,” Chemical Engineering Journal, vol. 388, art. 124320, 2020.

[12] M. Kohga, “Burning characteristics and thermochemical behavior of AP/HTPB composite propellant using coarse and fine AP particles,” Propellants, Explosives, Pyrotechnics, vol. 36, no. 1, pp. 57–64, 2011.

[13] S. Krishnan and R. Jeenu, “Combustion characteristics of AP/HTPB propellants with burning rate modifiers,” Journal of Propulsion and Power, vol. 8, no. 4, pp. 748–755, 1992.

[14] S. Xu, A. M. Pang, Y. Wang, X. Z. Pan, S. W. Li, H. T. Li, and J. Kong, “A review on the use of burning rate suppressants in AP-based composite propellants,” Propellants, Explosives, Pyrotechnics, vol. 47, no. 1, art. e202000327, 2022.

[15] S. Verma and P. A. Ramakrishna, “Activated charcoal: a novel burn rate enhancer of aluminized composite propellants,” Combustion and Flame, vol. 157, no. 6, pp. 1202–1210, 2010.

[16] Z. Li, N. Wang, B. Shi, S. Li, and R. Yang, “Effects of particle size on two-phase flow loss in aluminized solid rocket motors,” Acta Astronautica, vol. 159, pp. 33–40, 2019.

[17] C. Tu, X. Chen, F. Chen, Y. Zhuang, W. Cai, Y. Li, W. Li, C. Zhou, and R. Xie, “Effect of aluminum and ammonium perchlorate particle sizes on the condensed combustion products characteristics of aluminized NEPE propellants,” Scientific Reports, vol. 14, no. 1, pp. 1–18, 2024.